Chemistry & Biology
Resource

Visualization of Lipid Metabolism in the Zebrafish Intestine Reveals a Relationship between NPC1L1-Mediated Cholesterol Uptake and Dietary Fatty Acid

James W. Walters,[1] Jennifer L. Anderson,[1] Robert Bittman,[2] Michael Pack,[3] and Steven A. Farber[1,*]
[1]Department of Embryology, Carnegie Institution for Science, Baltimore, MD 21218, USA
[2]Department of Chemistry and Biochemistry, Queens College of the City University of New York, Flushing, NY 113[illegible] USA
[3]Department of Medicine, University of Pennsylvania, School of Medicine, Philadelphia, PA 19[illegible] USA
*Correspondence: farber@ciwemb.edu
DOI 10.1016/j.chembiol.2012.05.018

SUMMARY

The small intestine is the primary site of dietary lipid absorption in mammals. The balance of nutrients, microorganisms, bile, and mucus that determine intestinal luminal environment cannot be recapitulated ex vivo, thus complicating studies [illegible] absorption. We show that fluorescently labeled [illegible] can be used to visualize and study lipid absorpt[illegible] in live zebrafish larvae. We demonstrat[illegible] the a[illegible] tion of a BODIPY-fatty acid to a di[illegible] nigh[illegible] athe[illegible] genic lipids enables imaging [illegible] enter[illegible]cyte lip[illegible] droplet dynamics in real time. W[illegible] d-rich meal promotes BODI[illegible] choles[illegible]l absorption into an endosomal c[illegible]rtment d[illegible] quishable from lipid droplets. [illegible] show t[illegible]at dietary fatty acids promot[illegible] intestinal [illegible]esterol absorption by rapid re-loca[illegible]ation of NPC1[illegible] to the intestinal brush border[illegible] These d[illegible]a illustrate the power of the zebrafish syst[illegible] to address longstanding questions in vertebrate dig[illegible]ve ph[illegible]ology.

INTRODUCTION

Much of our understanding of intestinal lipid metabolism comes from studies that were not performed in the intestine but in immortalized cell lines (Field, 2001). The limitation of such experiments is that they cannot recapitulate the complex environment of living organs. The intestine, for example, is composed of multiple cell types, including enterocyte (ENT), stem, enteroendocrine, immune, and goblet cells (Field, 2001). In addition to its cellular heterogeneity, the intestine contains symbiotic organisms, bile, and mucus that each influence lipid processing (Field et al., 2003; Kruit et al., 2006; Martin et al., 2008; Moschetta et al., 2005; Pack et al., 1996; Titus and Ahearn, 1992). Because of the complexity of the intestinal environment and the lack of an equally complex ex vivo model, a number of questions remain regarding the uptake and compartmentalization of lipids in the polarized intestinal epithelial cell, the ENT.

Within intestinal lumen, dietary lipids (cholesterol, plant sterols, phospholipids, and triglycerides) are digested by luminal lipases and bile, processing mixed micelles (Iqbal et al., 2008). From the surface of micelles, monoacylglycerol and fatty acids (FA) are readily absorbed by ENTs in the proximal small intestine (Benzonana and Desnuelle, 1965; Iqbal et al., 2008; Sarda and Desnuelle, 19[illegible] Despite years of study, the detailed roles of proteins (e.g. FATP4 and/or CD36) that mediate the initial steps of lipid FA absorption by intestinal ENTs is not known (Mansbach and Gorelick, 2007).

Once FA enter the ENT, they are rapidly directed to the endoplasmic reticulum (ER), where they are re-esterified into triacylglycerides (TG) (Jersild, 1966; Lehner and Kuksis, 1995; Nutting et al., 1989). The ENT will either transfer the TG to maturing lipoproteins (chylomicrons) destined for the Golgi and subsequent basolateral exocytosis or incorporate TG into lipid droplets (LD) that are thought to arise by budding from the ER (reviewed by Iqbal and Hussain, 2009; Mansbach and Siddiqi, 2010). Isotopic labeling studies of rat ENTs indicate that the rate-limiting step in TG export is transfer of TG from the ER to the Golgi (Mansbach and Nevin, 1998). These data suggest that storage of TG would be favored over TG export when intestinal FA levels are high and are consistent with the appearance of large numbers of intestinal LDs following a high-fat meal in mice, zebrafish, and trout (Weiss, 1955; Sire et al., 1981; André et al., 2000). However, much of our information about the cell biology of LD comes from studies of adipocytes and not ENTs. Specifically, we do not know how ENTs regulate LD production.

Cholesterol absorbed by ENTs is incorporated into lipoproteins destined for export into the lymphatic system. Neimann-Pick C1-like 1 (NPC1L1) protein plays a key role in intestinal cholesterol absorption, as rodents lacking NPC1L1 fail to uptake cholesterol (Altmann et al., 2004; Klett and Patel, 2004). In addition, NPC1L1 expression is enhanced in humans treated with cholesterol synthesis inhibitors (Tremblay et al., 2011) and down-regulated in cultured cells subjected to prolonged oleic acid (FA, C18:1) exposure (Chen et al., 2011). In intestinal explants, NPC1L1 responds to cholesterol in the culture media by translocating from the brush border (BB) to an endosomal compartment (Skov et al., 2011). Sterol-induced internalization of NPC1L1 from the plasma membrane into the endosomal compartment of rat CRL-1601 hepatocytes can be blocked by clathrin/AP2 knockdown and the drug ezetimibe (Ge et al., 2008). Although this suggests an integral role for NPC1L1 in cholesterol absorption and trafficking, there is no cell biological model to explain how specific intestinal proteins uptake cholesterol from the

intestinal lumen or how NPC1L1 is involved in this process. Moreover, it is unclear to what degree the observations of NPC1L1 translocation in cultured cells will apply to the highly specialized environment of the intestine.

The finding that fat consumption can promote intestinal cholesterol uptake needs elucidation. Sylvén and Borgström (1969) found that TG comprised of long fatty acyl chains enhances uptake of cholesterol in rats. Mice lacking pancreatic lipase have significantly reduced levels of luminal FA and exhibit reduced cholesterol absorption (Young and Hui, 1999). More recently, absorption of long-chain FA (LCFA) was found reduced in mice deficient in NPC1L1 and in ezetimibe-treated mice and zebrafish larvae (Labonté et al., 2008; Clifton et al., 2010). As cholesterol and fat are always found in combination in natural diets, it may not be surprising that FA liberated from TG breakdown could play a role in cholesterol absorption. However, the mechanism whereby dietary FA modulates cholesterol metabolism has not yet been described.

To address outstanding questions regarding mechanisms of intestinal lipid absorption, we have developed a strategy for visualizing lipids and relevant proteins at a subcellular level within ENTs of live zebrafish larvae. One reason for the po[illegible]ity of the zebrafish system is that adults are small, highly fec[illegible] v[illegible]brates that produce large numbers of developmentally [illegible]chro[illegible]nized progeny. Moreover, the biochemistry and physio[illegible] zebrafish are similar to humans in many re[illegible]owing t[illegible]eir small size, many larvae can be simult[illegible]ously [illegible]nipulat[illegible]n multiwell plates under a variety of co[illegible]ons (e[illegible]temperat[illegible]e, diet, and pharmacology). The optical cla[illegible] [illegible]e lar[illegible] facilitates the use of fluorescently l[illegible]led lipid[illegible]ophilic dyes, and fluorescent fusion proteins t[illegible]nitor subcell[illegible]vents without surgical or other invasive [illegible]oce[illegible]es. Together, these features have resulted in the rapid, world[illegible] adoption of this model vertebrate system.

Previous wo[illegible] examin[illegible]g zebrafish lipid processing was largely perfo[illegible]d at l[illegible] magnification (1–5× objective) with a focus on org[illegible]tion (B[illegible] et al., 1997; Durliat et al., 2000; [illegible] et a[illegible]003; [illegible]ma et al., 2009; Hendrickson et a[illegible]999; [illegible]o et a[illegible]; Hölttä-Vuori et al., 2010; Marza e[illegible], 2005; [illegible]g et al., 2[illegible]05). Here, we describe a method for hig[illegible] so[illegible] of intestinal cells under different dietary cond[illegible] and after exposure to small molecules known to affect li[illegible] metabolism in humans. Our method employs commercia[illegible]available fluorescent lipids for direct observation of lipid absorption at the subcellular level in the intact intestine and does not require specialized equipment beyond a confocal microscope and imaging software.

Using this approach, postprandial lipid processing was monitored visually at a subcellular level in real time. We find LDs form rapidly in larvae fed a high-fat diet and that absorption of cholesterol by ENTs requires the presence of dietary FA. Additionally, fluorophore-conjugated FA label LDs and are visible by both phase and fluorescence microscopy. We observed that BODIPY-cholesterol is initially taken up in an endosomal compartment that is distinct from newly formed LDs. In addition, a high-fat diet causes fluorescently tagged human NPC1L1 to translocate to the intestinal BB from its resident perinuclear compartment. The results suggest that, in vivo, NPC1L1 promotes cholesterol absorption in response to signaling from free FA.

RESULTS

Intestinal Lipid Droplets Result from a High-Fat Meal

To establish larval zebrafish as a model for studying transport and metabolism of dietary lipid, w[illegible]lected a high-fat food that easily forms an emulsio[illegible]water. v[illegible]und that fresh chicken egg yolk (EY; approxi[illegible]y 60% TG, [illegible]% phospholipids, and 5% cholesterol) forms [illegible]iform em[illegible]sion of small micelles when mixed wi[illegible]ebrafish [illegible]rvo [illegible]lia (EM) (10% v/v) by force pipettin[illegible]when i[illegible]mersed[illegible]e solution, freely swimming larvae r[illegible]y co[illegible]e the high-fat diet. Normally, zebrafish begin [illegible]ating [illegible]nous fo[illegible]between 4 and 6 days post-fertilizati[illegible](dpf) as[illegible]y de[illegible]e their yolk nutrients. In these exp[illegible]ts, the EY e[illegible]was the larva's first exogenous foo[illegible]ur[illegible]fter 3 hr of fe[illegible]ding, the anterior larval intestine of most larvae (~9[illegible]was full of EY, as evidenced by its opaque a[illegible]nce when c[illegible]ared to unfed siblings (Figures 1A and [illegible]).

Ultrastructural analysis of the intestinal ENTs of zebrafish [illegible]rvae revea[illegible]features strikingly similar to those previously [illegible]erved in [illegible]man and mouse intestines (Ashworth and Law[illegible]Marenus and Sjöstrand, 1982). The zebrafish intestine at 6 dpf consists mainly of uniform, columnar, polarized [illegible]lia, with an apical BB, lateral cell border, and basal basement membrane. The apical ENT cytoplasm contains copious spherical mitochondria and SER (Figure 1C). The most notable effect of feeding the high-fat diet to larvae was the rapid appearance of large lipid accumulations filling most of the ENT's apical cytoplasm adjacent to the BB (Figures 1D–1F). These accumulations were determined to be LD by their uniform interior, association with ER and mitochondria, and presence of a bounding monolayer membrane (Figure 1E). Fed larvae also exhibited chylomicron particles in the basolateral compartment of their ENTs (Figure 1D) and a dramatic change in mitochondria morphology. Some mitochondria appeared to undergo fusion that resulted in a shift to long, tubular shapes (compare Figures 1G and 1H), a response only observed in ENTs from fed larvae. To test whether these observations were specific to a high-fat intake, a natural diet of 3% puréed baby brine shrimp was fed overnight. This lower-fat diet also produced LDs, chylomicrons, and changes in mitochondria morphology, although the effects were less dramatic (data not shown).

To better understand the kinetics of ENT LD formation and utilization, we performed time-course studies in which larvae were fed for a specific duration, fixed, and subjected to ultrastructural analysis. These studies revealed that a brief high-fat feed (1 hr) produced a peak in LD area at 1 hr post feed that was maintained (over 9 hr; Figure S1B [available online], $p = 2.6x10^{-7}$, $R^2 = 0.565$) and gradually reduced (from 9–21 hr) to return to baseline (Figure S1D, $p = 0.004$, $R^2 = 0.794$).

BODIPY-Labeled FAs Are Incorporated into LDs in the Enterocyte

Although a major function of ENTs is to uptake dietary lipids for absorption into the body, the subcellular trafficking of intestinal lipids has not been examined in live animals. To explore the dynamics of intestinal lipid processing, we exploited the optical clarity of larval zebrafish and developed methods to visualize subcellular lipid within live ENTs through the use of

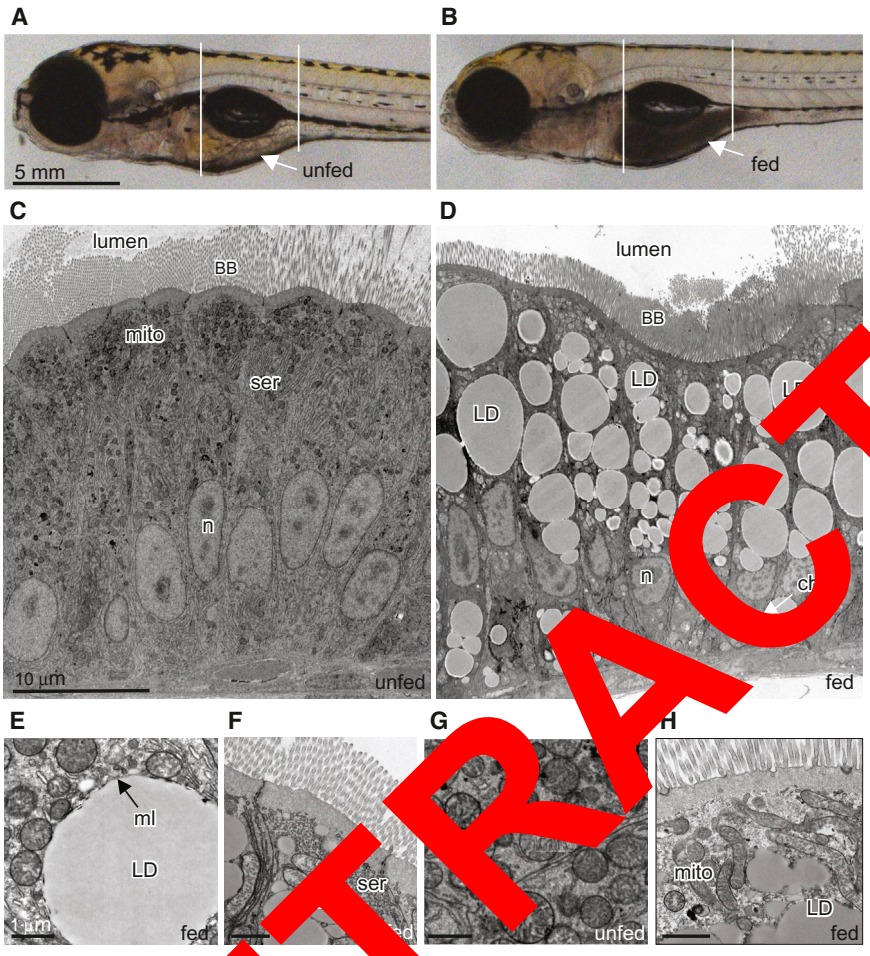

Figure 1. Lipid Droplets Form in Zebrafish Enterocytes after a High-Fat Meal

(A and B) Brightfield image of (A) unfed and (B) fed (10% chicken EY, 3hr) zebrafish larva (6 dpf). Arrows indicate intesti[nal bulb] and reveal the region of food accumulati[on]; [lines] demarcate the anterior intesti[nal] area where [studies focused. (C–H) Electro[n micro]graphs fro[m] unfed and fed zebrafish larvae [as] shown. (C) [Unfed] zebrafish intesti[nal] ENTs lack [lipid] droplet[s] (LD). (D) Zebrafish ENTs from larvae [that] have been fed chicken EY (10%, 8 hr) display ma[ny] LD. (E) Characteristic photoreceptor monolayer (ml) bound a lipid droplet. (F) [The] endoplasmic reticulum (ser) is closely associated with [lipid] droplets. Lipid droplets are observed [in the] apical brush border following feeding. (G) Spherical mitochondria are typical in unfed ENTs. (H) ENTs from larvae fed as described in (D) typically have fused mitochondria (mito) closely associated with lipid droplets.

BB, brush border; n, nucleus; LD, chylo, chylomicron. See also Figure S1.

fluorophore-labeled lipids. To track TG, a major constituent of LDs, a fluorescent FA analog (BODIPY-C12) was added to the EY diet and fed to larvae. Confocal microscopy of these larvae revealed a fluorescently labeled subcellular compartment that closely paralleled the size, shape, and distribution of LDs observed in electron micrographs (compare Figure 2B and Figure 2W). We used confocal microscopy to visualize LDs and found that they colocalized with the BODIPY-C12 spheres (Figure S2). Larvae fed BODIPY-C12 without EY exhibited diffuse and weak cytoplasmic fluorescence but no LDs, presumably because the FA content of the BODIPY-C12 diet was at low molar amounts compared to the BODIPY-C12 plus EY diet (Figures 2A and 2C and Figure S2). This experiment indicates that LDs can be visualized in live larvae using an optimized diet, optimized mounting procedure (Figure S3), 63× oil immersion objective, and standard confocal microscope.

Studies of cultured cells have shown that LDs are enriched in sterols and sterol esters (Garbarino et al., 2009; Le Lay et al., 2006; O'Rourke et al., 2009). To determine whether dietary cholesterol partitions to intestinal LDs following its uptake, we used a cholesterol molecule with a BODIPY analog conjugated to the side chain at carbon-24 (BODIPY-cholesterol) (Li et al., 2006). This fluorescent cholesterol analog localizes to the liquid-ordered domain within membranes, mimicking the behavior of native cholesterol (Bidet et al., 2011; Marks et al., 2008; Sankaranarayanan et al., 2011; Wüstner et al., 2011). We examined ENTs from larvae fed BODIPY-cholesterol with EY and found that the subcellular fluorescent labeling did not overlap with LDs (Figure 2E). In addition, when larvae ingested BODIPY-cholesterol in the absence of EY, the cholesterol analog was not taken up by ENTs (Figure 2D). In fact, we observed virtually no cytoplasmic fluorescence in larvae fed BODIPY-cholesterol alone (Figure 2F; two-tailed t test, $p = 0.048$). To test the hypothesis that BODIPY-cholesterol is insoluble without EY, we subjected the labeling solution to centrifugation (Figures S4A and S4B). The failure of BODIPY-cholesterol to form a pellet suggests that a stable emulsion is formed when it is added to EM. To rule out the possibility that a failure to uptake BODIPY-cholesterol was due to insolubility or a failure of bile to be secreted, we dissolved BODIPY-cholesterol in fish bile and found that cytoplasmic fluorescence in the ENT was not enhanced (Figure S4C).

BODIPY-Cholesterol Absorption Is Dependent on Luminal Long-Chain FA

One possible reason for the failure of ENTs to uptake BODIPY-cholesterol was that, when given alone, the physiologic responses that would normally initiate a cascade of digestive processes necessary for cholesterol absorption do not occur. To test this, we added BODIPY-cholesterol to chicken egg white, a high-protein, very low-lipid (less than 0.2% by weight) food (U.S. Department of Agriculture, Agricultural Research Service, 2011). When fed to 6 dpf larvae, ENTs displayed strikingly lower cytoplasmic fluorescence intensity than those in larvae fed with the BODIPY-cholesterol and EY diet (ANOVA with Games-Howell, $p = 0.023$) (Figures 3A and 3C). These data suggest that a component of the EY is required for BODIPY-cholesterol absorption.

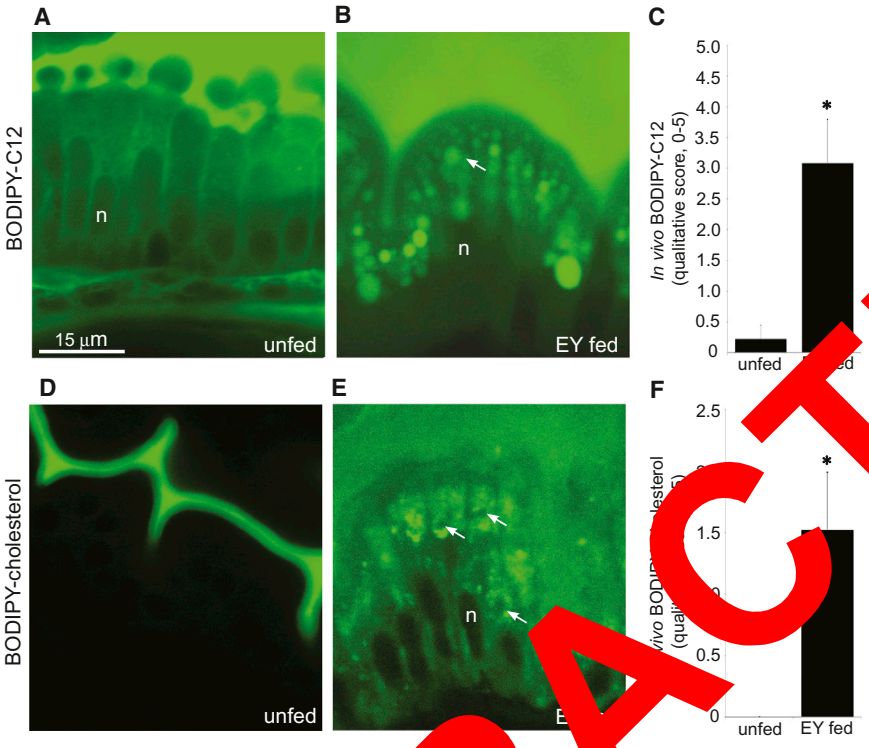

Figure 2. Larvae Fed a High-Fat Meal Containing BODIPY-Lipid Analogs Exhibit Robust and Discrete Subcellular Fluorescence within Enterocytes

(A–D) Confocal ima (63×) of live ENTs treated with different di s and labeled with either BODI 12 or BO -cholesterol. (A) ENTs are ely labeled BODIPY-C12 is su lied t fed larvae. BODIPY-C12 lab rge sphe ipid d ts (arrow) when d to a high-fat chicken EY in EM). BODI 12 label of ENTs is enhanced the ence of food. Plotted are mean ± SE ree inde ent experiments. Images (as and were blindly scored for cytoplasm cence on a five point qualitative scale, wh 5 represents strong and abundant signal and 0 represents no signal. Data were analyzed using two-tailed t test for equality means. *p < 0.05. (D) ENTs are not labeled when BODIPY-cholesterol is supplied to unfed larvae.

(E) When added to a high-fat meal, BODIPY-cholesterol reveals a cholesterol-bearing compartment distinct from lipid droplets (compare to B). Arrows indicate negatively stained lipid droplets.

(F) BODIPY-cholesterol labeling of ENTs requires the presence of food. Plotted are mean ± SE from three independent experiments. Images (as in D and E) were blindly scored for cytoplasmic fluorescence on a five point qualitative scale, wh represe strong and undant signal and 0 represents no signal. Data were analyzed using two-tailed t test for equality of means. *p < 0.05.

n, nucleus; EY, chicken EY. See also F es S2 .

Approximately 60% pid the EY die are TGs that cannot be absorbed irectly but t be digested by luminal lipases to free FA a mono- and dig ides that can be taken into ENTs. We t ed if c lesterol abs rption requires luminal FA by exami the ct of adding the TG lipase inhibitor Orlistat (1 mM) BODIP cholesterol/EY emulsion. By inhibiti action umin ases, dietary TGs are no longer clea into e FA a o- and diglycerides. ENTs treated w Orlistat d fed the ODIPY-cholesterol/EY diet exhibited no ifi in cytoplasmic fluorescence compared to th ed the BODIPY-cholesterol/egg white diet (Figures 3A, 3D, d 3E) (ANOVA with Games-Howell; EW versus EY+Orlistat > 0.05). These findings indicate that BODIPY-cholesterol absorption requires the presence of free FA and/or diacyl- or monoacylglycerol. To determine if FA are the components in TG required for cholesterol uptake, oleic acid (C18:1) was added to the fatty-acid free BODIPY-cholesterol/egg white emulsion and fed to 6 dpf larvae. These larval ENTs displayed a substantially higher BODIPY-cholesterol fluorescence intensity in their cytoplasm (Figures 3B and 3E). We confirmed that this observation was not due to auto-fluorescence produced by C18:1 by assaying and found no intestinal fluorescence in larvae fed C18:1 and egg white in the absence of BODIPY-cholesterol (data not shown). Moreover, while a diet of C18:1 and BODIPY-cholesterol/egg white emulsion did not produce as many LDs as the BODIPY-cholesterol/EY diet, it produced a similar level of cytoplasmic fluorescence (Figure 3E) (ANOVA with Games-Howell, EY versus C18:1, $p > 0.05$), supporting our observations that efficient BODIPY-cholesterol absorption requires FA.

Having established that adding C18:1 to the larval diet promotes cholesterol uptake, we then tested if this effect was specific to LCFA or if it would be observed by feeding any exogenous FA. Thus, we performed the assay with FA of various chain lengths and found that adding C16:0 to the egg white/BODIPY-cholesterol emulsion significantly enhanced ENT fluorescence compared to egg white/BODIPY-cholesterol alone (Figure 3H) (ANOVA with REGWQ, $p < 0.001$, ~25% of the effect obtained with C18:1). FA of other chain lengths did not significantly enhance BODIPY-cholesterol uptake ($p > 0.05$). The ability of hydrolysis products of TG other than free FA (diacylglycerol, monoacylglycerol, and glycerol) was also assayed for their ability to enhance dietary BODIPY-cholesterol uptake. Only 1,2-dioleoyl-*rac*-glycerol, a molecule that contains two oleic acid molecules that are likely liberated by digestive enzymes, showed a significant effect (Figure 3I) (ANOVA with REGWQ, $p = 0.002$). These studies support the hypothesis that a long-chain FA is essential for BODIPY-cholesterol absorption.

A fluorescently labeled lipid may be processed differently than the unmodified lipid. To address the degree to which dietary BODIPY-cholesterol is analogous to native cholesterol, we mixed radiolabeled cholesterol (16.6 μCi of [^{3}H]-cholesterol/20 larvae/tube) with chicken egg white. Since this is significantly less cholesterol (3.53 μM) than BODIPY-cholesterol (100 μM) that was routinely used in our studies, we added unlabeled cholesterol to the egg white/[^{3}H]-cholesterol emulsion so that

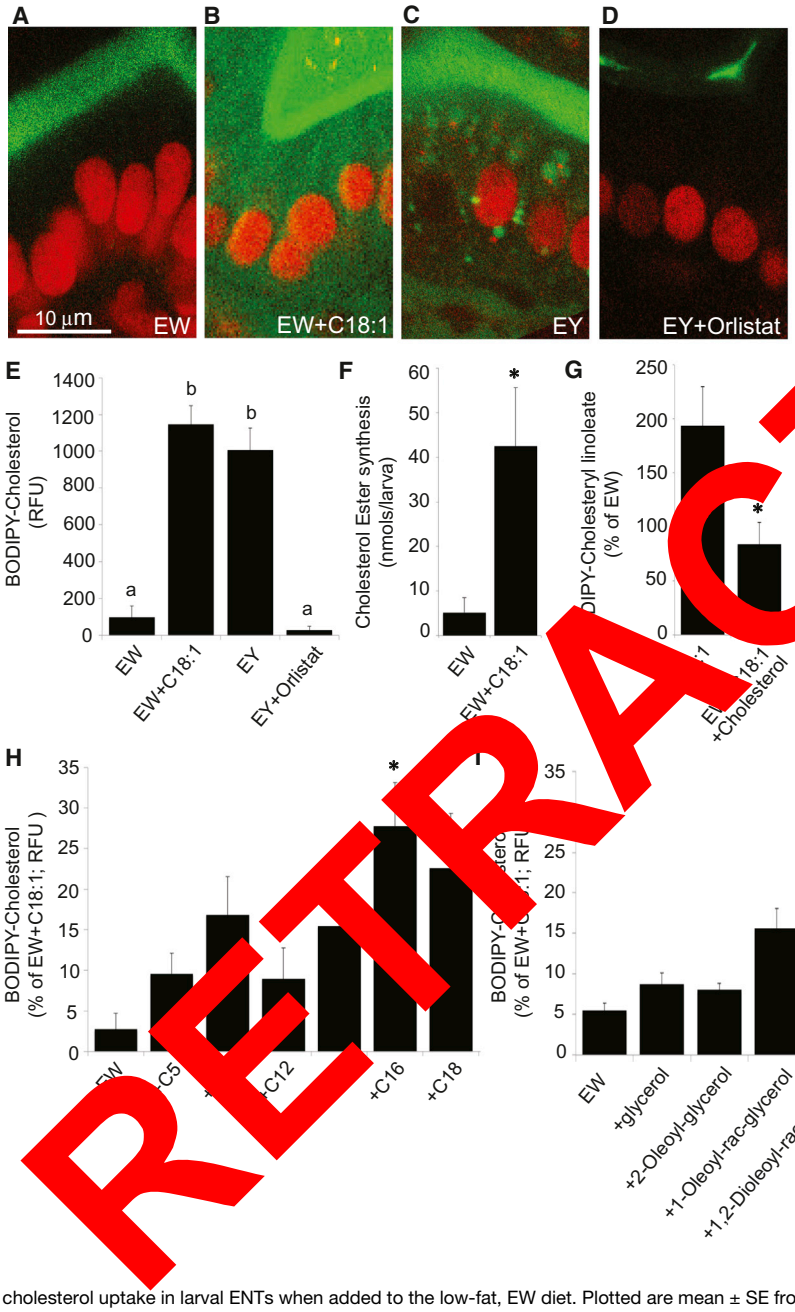

Figure 3. Intestinal Absorption of BODIPY-Cholesterol by Larval Enterocytes Requires the Presence of Fatty Acid

(A–D) Confocal images (63×) showing BODIPY-cholesterol (green) fluorescence in live 6 dpf larval ENTs (expressing mCherry nuclear marker [red]) under different conditions. (A) ENTs from larvae fed protein-rich, low-fat diet (EW: 5% chicken egg white) do not take up BODIPY-cholesterol although abundant in the lumen. (B) ENTs from larvae fed EW+C18:1 (1 mM) show increased uptake of BODIPY-cholesterol. (C) ENTs from larvae fed a high-fat diet (EY: 5% chicken egg yolk) take up BODIPY-cholesterol. (D) ENTs from larvae pretreated with the pancreatic lipase inhibitor Orlistat (1 mM) show no BODIPY-cholesterol uptake although it is abundant in the lumen.

Relative BODIPY-cholesterol fluorescence (relative fluorescence units [RFU]) in live larval ENTs from treatments with and without available FA. Both the EY diet and the EW plus C18:1 diet significantly enhance BODIPY-cholesterol uptake. Plotted are mean ± SE from three independent experiments. Means with different letters (a,b) are statistically different: $p < 0.05$ from ANOVA with Games-Howell.

(F) Adding FA C18:1 added to the EW diet of larvae results in a substantial increase in [^{3}H]-cholesterol ester synthesis as measured by TLC. Plotted are mean ± SE from four independent experiments. Data were analyzed using two-tailed t test for equality of means. *$p < 0.05$.

(G) Addition of unlabeled cholesterol (100 µM) to the BODIPY-cholesterol/EW/C18:1 emulsion significantly reduced BODIPY-cholesterol ester (BODIPY-cholesteryl linoleate) synthesis. Plotted are mean ± SE from three independent experiments, presented as a percentage of the EW treatment results. Data were analyzed using two-tailed t test for equality of means. *$p < 0.05$.

(H) Addition of C16:0 to the low-fat EW diet significantly enhances BODIPY-cholesterol uptake into larval ENTs. Other FA tested did not significantly enhance BODIPY-cholesterol uptake when added to the EW diet. Plotted are mean ± SE from four independent experiments, presented as a percentage of the EW+C18:1 treatment results. *$p < 0.05$ from ANOVA with REGWQ.

(I) The hydrolysis product of TG, 1,2-dioleoyl-*rac*-glycerol, significantly enhances BODIPY-cholesterol uptake in larval ENTs when added to the low-fat, EW diet. Plotted are mean ± SE from three independent experiments, presented as a percentage of the EW+C18:1 treatment results. *$p < 0.05$ from ANOVA with REGWQ.

See also Figure S4.

the final molar concentrations were equivalent across studies. Since it is not possible to remove the unincorporated cholesterol from the larval intestine, we assayed the formation of cholesterol ester by thin layer chromatography (TLC). Addition of C18:1 to the egg white diet resulted in a substantial increase in cholesterol ester synthesis (Figure 3F) (two-tailed t test, $p = 0.018$). This is in contrast to total cholesterol ingested, of which we observed no significant difference between the treatment groups: the total cholesterol ingested (determined from the total radioactivity recovered/ specific activity of the labeling solution) between the egg white diet and egg white plus oleic acid diet groups was 996 ± 429 versus 1220 ± 252 nmol/larva, respectively (mean ± SEM, $p > .05$). These results suggest that animals swallow approximately equivalent amounts regardless of specific diet.

To further assess the degree to which BODIPY-cholesterol is processed similarly to cholesterol, we explored the degree to which unlabeled cholesterol can compete with BODIPY-cholesterol for esterification. The addition of cholesterol (100 µM) to the BODIPY-cholesterol/egg white/C18:1 emulsion reduced BODIPY-cholesterol ester formation by approximately 50% (Figure 3G) (two-tailed t test, $p = 0.007$). While both cholesterol

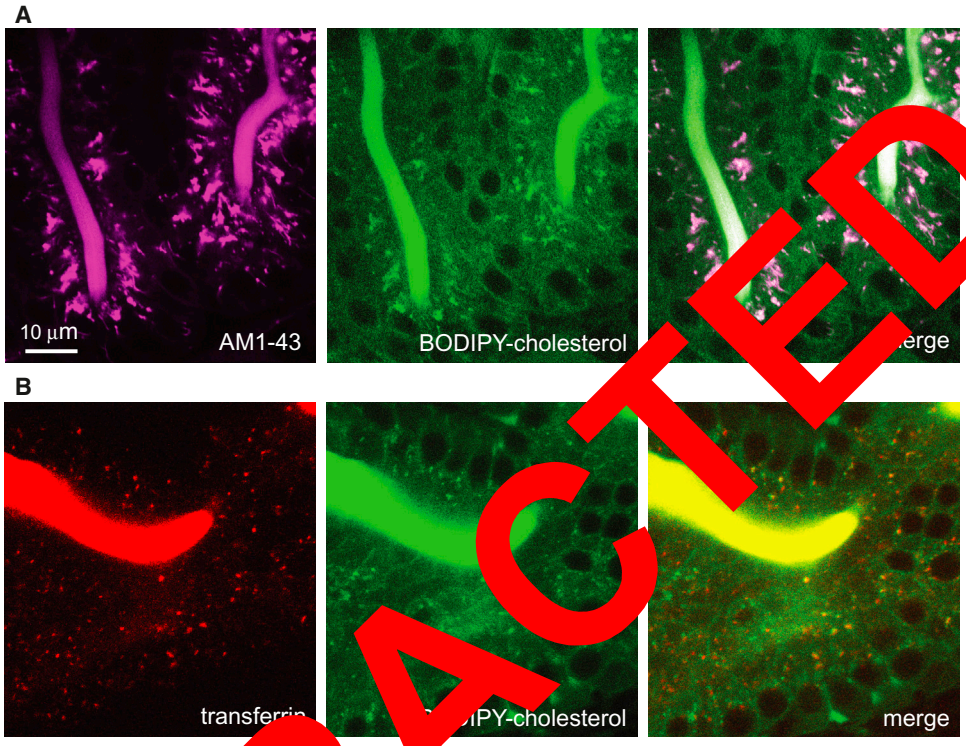

Figure 4. BODIPY-Cholesterol Accumul within Endocyt ompartment that Is Distinct from Lipid Droplets

(A and B) Confocal images (63×) showing tra n-Ale (transferrin) or AM1-43 labeling of the endocytic compartment in live 6 dpf larval ENTs. All larvae were fed a high-fat diet containin ODIP erol. Eac ge is representative of images taken from three or more experiments. (A) AM1-43-labeled endocytic compartments (magenta) alize with PY-cholesterol labeled enrichments (green) during feeding. Adjusted PCC in ROI = 0.46; thresholded $M_{A,\ AM143}$ = 0.95; thresholded M_B = 0.99. (B) Tra in-labeled endocytic compartments (red) co-localize with BODIPY-cholesterol labeled enrichments (green) during feeding. Adjust CC ol volume = 0.2 hresholded $M_{A,Tf555}$ = 0.89; thresholded $M_{B,Tf555}$ = 0.84.

and BODIPY-cho erol are este we observed less BODIPY-choles l ester rmation tha radioactive cholesterol ester (as a pe t of s trate; data not shown). However, after a significantly lo riod of ding (12–15 hr), we observed numer ODIPY lest positive LDs (data not shown), cons ent v even erification of BODIPY-cholesterol a ncorpo ion to LD . These data suggest that BODIPY-ch ter n is likely slower than unmodified chole l.

To fu explore metabolism of BODIPY-cholesterol, we examined effect of an ezetimibe analog (SCH58053), a compound known to inhibit mammalian cholesterol uptake. In zebrafish larvae, SCH58053 (50 μM) could completely block the FA induced uptake of BODIPY-cholesterol by intestinal ENTs (egg white alone, 107 ± 32 RFU; egg white + oleic acid, 1596 ± 238 RFU; egg white + oleic acid + SCH58053, 35 ± 25 RFU; mean ± SEM, n = 4 experiments, three larvae per experiment; ANOVA with Games-Howell, $p < 0.05$). Taken together, these data are consistent with the hypothesis that BODIPY-cholesterol is taken up and metabolized similar to native cholesterol.

BODIPY-Cholesterol Localizes to the Endocytic Compartment of Enterocytes

To identify subcellular structures labeled by BODIPY-cholesterol, we compared its localization with cytoplasmic fluorescence of the styryl dye AM1-43. FM dyes, of which AM1-43 is a fixable derivative, are well-established markers for the endocytic pathway and emit fluorescence only when intercalated into lipid bilayers (Babitt et al., 1997; Betz et al., 1992; Choudhury et al., 2002; Davies and Ioannou, 2006; Diefenbach et al., 1999; Kuromi and Kidokoro, 2005; Le Lay et al., 2006; Murthy and Stevens, 1998). We previously used AM1-43 to study lipid absorption and trafficking defects in zebrafish larvae (Clifton et al., 2010; Ho et al., 2006). The spectral properties of AM1-43 (excitation maximum at 479 nm, emission maximum at 598 nm) and BODIPY (excitation, 505 nm; emission, 511 nm) enabled us to resolve the two fluorophores with minimal overlap. Larvae (6 dpf) that had ingested AM1-43 with a BODIPY-cholesterol/EY emulsion for 3 hr exhibited a high degree of co-localization between regions of cytoplasmic fluorescence (adjusted PCC in ROI volume = 0.46; thresholded $M_{A,\ AM143}$ = 0.95; thresholded $M_{B,\ AM1-43}$ = 0.99) (Figure 4A). Control larvae were labeled with either AM1-43 or BODIPY-cholesterol to correct for potential channel crossover (negligible; data not shown).

To further support these findings, we employed transferrin, a marker that is internalized via clathrin-mediated endocytosis. We pretreated larvae with a protease inhibitor cocktail to reduce the activity of luminal proteases that would normally digest transferrin. We then fed the larvae a BODIPY-cholesterol/EY emulsion and transferrin-Alexa Fluor 555 (for 3 hr) (Roche Diagnostics). We observed a high degree of co-localization between

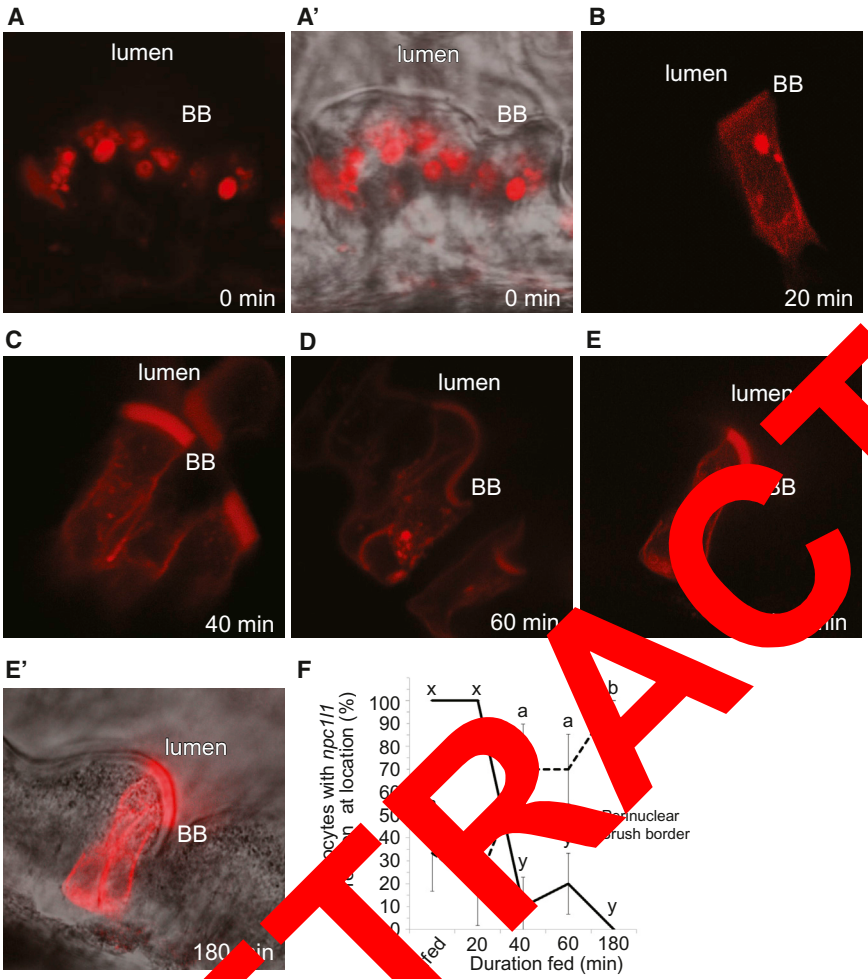

Figure 5. Human NPC1L1 Mobilizes from a Perinuclear Structure to the Brush Border in Larval Enterocytes Fed a Lipid-Rich Meal

(A–E') Representative clones of *hsp70-hnpc1L1-mCherry* in 6 dpf l... (three independent experiments, 12 a...), ...me course begins 3 hr after a 15 ... heat-shoc... before exogenous food ... ovided. (A) ...ore a feed, *HsNPC1L1-mCh...* is enriched ... a spherical perin... structu... Overl... A with phase im... (B–E) *HsNPC1...* ...ry becomes enr... ed pred...antly on t... ush border (BB) and ...ted ... the perinuclear structure during an EY ...g. (E') Ov... of (E) with phase image.

(F) h... L1-m...ry relocalizes from a perinuclear ... (solid line) to the brush border (dashed lin... during feeding of a lipid-rich meal. Plotted are mean ± SEM from five independent ...eriments. Means with different letters (a,b or x...e statistically different: $p < 0.05$ from ANOVA with REGWQ (perinuclear, x and y) or Games-Howell (brush border, a and b).

BODIPY-choles... and ...nsferrin-Alexa Fluor 555 (adjusted PCC in ROI volum... 6; thres...ded $M_{A,Tf555} = 0.89$; thresholded M... 0.84)... ese d... indicate that BODIPY-cholesterol i...ansp...ed with ...osomes during the uptake phase of ...esterol ...sorption.

NPC1L... ...sponds to Increased Levels of Free FA

To elucid... ...he mechanism of FA dependence on BODIPY-cholesterol u...ke we characterized the localization of a human NPC1l1-mCherry fusion protein after EY feeding. Design of the transgene was based upon a previously validated human *NPC1L1-eGFP* transgene (Ge et al., 2008). Temporal control of transgene expression was afforded by use of a heat shock promoter, *hsp70* (Ish-Horowicz et al., 1977). To minimize confounding effects of overexpression, we tested a range of heat-shock durations to identify the least amount of time that resulted in detectable levels of fluorescence (15 min at 37°C). Transgenic larvae (F0, 6 dpf) were fed an EY diet and subjected to confocal microscopy at various time points. Because of the mosaic nature of exogenous plasmid incorporation, only a small number of clones would be expected to express the transgene. Before food was supplied (3 hr after heat shock), intracellular NPC1L1-mCherry fluorescence within ENTs was confined to spherical cytoplasmic structures adjacent to the nucleus (Figures 5A–5A'). Intriguingly, within 40 min after a high-fat meal, we observed a pronounced re-localization of *Hs*NPC1L1-mCherry to cell membranes, with significant enrichment at the BB membrane over time (Figures 5B–5F). After 3 hr of feeding, NPC1L1-mCherry was dispersed from spherical cytoplasmic structures adjacent to the nucleus (ANOVA with REGWQ, $p < 0.05$) and 100% of the clones exhibited BB fluorescence (ANOVA with Games-Howell, $p = 0.034$; in contrast to only 20% of the unfed clones) (Figure 5F).

To evaluate if FA derived from TG breakdown mediates the redistribution of *Hs*NPC1L1, larvae were treated with Orlistat. After an EY feed (3 hr), a significant amount of NPC1L1 remained concentrated in the cytoplasm in Orlistat-treated larvae (ANOVA with REGWQ, $p < 0.05$) (Figures 6A and 6B). To test the hypothesis that FA are the TG catabolites that mediate the redistribution of NPC1L1, C18:1 was added to the egg white emulsion and fed to 6 dpf larvae. The larval ENTs displayed substantial NPC1L1-mCherry fluorescence on their BB membranes and dispersed throughout the cytoplasm (Figures 6A and 6B). These data suggest that subcellular localization of NPC1L1 localization is influenced by dietary FA.

Having established that both NPC1L1 localization to intestinal BB and cholesterol uptake by ENTs is correlated with the presence of dietary FA, we set out to test if NPC1L1 could directly mediate BODIPY-cholesterol uptake without the presence of dietary FA. A stable line containing the *hsp70: HsNPC1L1-mCherry* construct was made. We took advantage of the control afforded by the heat shock promoter to increase the levels of NPC1L1-mCherry, with the goal of forcing some NPC1L1-mCherry to the BB. In contrast to our short heat shock (15 min), low-expressing NPC1L1-mCherry experiments (Figures 5, 6A, and 6B), we increased the duration of heat shock four-fold (1 hr) to induce high expression. This resulted in

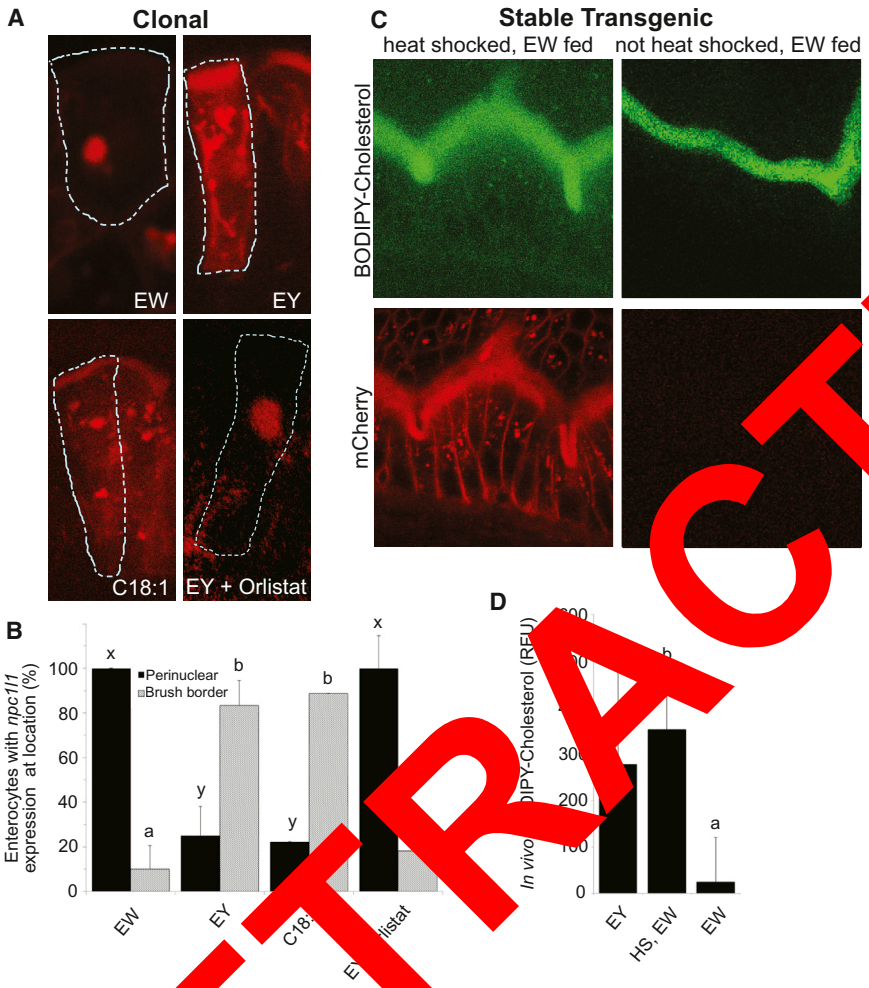

Figure 6. NPC1L1 Directly Mediates BODIPY-Cholesterol Uptake by Larval Enterocytes

(A) Representative cells in larvae fed egg white (EW) expressing *Hs*NPC1L1-mCherry (6 hr after a 15 min heat-[illegible] after feeding) are outlined in 6[illegible]arval ENTs. NPC1L1-mCherry accumulate[illegible] a perinuclear location. This contrasts with[illegible]brush border accumulation of *Hs*[illegible]L1-mCh[illegible] clone[illegible]ithin larvae fed [illegible] chicken egg y[illegible]EW plus C18:1 for [illegible]e same[illegible]ation. Similarly, clones in Orlistat-[illegible]ated[illegible]fed larvae do not show re-localization [illegible]holesterol[illegible]sporter to the brush border. (B) [illegible]l ENT[illegible]d the EY and EW+C18:1 diets display[illegible]sNPC1L1-mCherry at their brush border co[illegible]pared to those fed the EW and EY+Orlistat diets which show significant perinuclear [illegible]richment. Plotted are mean ± SEM from six [illegible]ependent experiments. Means with different letters (a,b or x,y) are statistically different: $p < 0.05$ from ANOVA with REGWQ (brush border, a and b) or Games-Howell (perinuclear, x and y).

(C) ENTs from stable hsp70-*Hs*NPC1L1-mCherry lines (red) that were heat-shocked (1 hr), allowed to recover (3 hr), and then fed EW+BODIPY-cholesterol (green). Strong overexpression of *Hs*NPC1L1-mCherry causes the cholesterol transporter to be localized to the brush border causing BODIPY-cholesterol to be transported into ENTs.

(D) Heat shock of larvae from *Hs*NPC1L1-mCherry stable lines provides significant uptake of BODIPY-cholesterol into ENTs. Relative fluorescent units (RFU) of BODIPY-cholesterol in larval ENTs under conditions of EY-fed with no heat shock; heat-shocked (HS), EW-fed; and EW fed conditions. Plotted are mean ± SEM from four independent experiments. Means with different letters (a,b) are statistically different: $p < 0.05$ from ANOVA with REGWQ.

npc1l1, Niemann-Pick C1-like 1.

NPC1L[illegible]erry l[illegible]izatio[illegible] both the BB and the spherical cyto[illegible]smic structur[illegible]en these larvae were fed the B[illegible]PY-ch[illegible]sterol/egg white diet they exhibited a significant in[illegible]e[illegible]holesterol fluorescence (ANOVA with REG[illegible] $p < 0.05$), compared to EY feeding (and in contrast to transge[illegible]nimals that were not subjected to heat shock and WT contro[illegible]mals subjected to heatshock [data not shown]) (Figures 6C and 6D). These data indicate that the localization of NPC1L1 to the BB membrane is sufficient to promote cholesterol uptake.

DISCUSSION

A fundamental step to understanding the mechanisms of FA and cholesterol uptake by intestinal ENTs is to observe lipid absorption at the subcellular level in a live organism. Previous reports of cellular lipid absorption have been limited by an inability to recreate the complex in vivo milieu of the intestinal lumen. In addition, ex vivo studies lack a variety of physiological processes impacting intestinal function at both the whole organ and subcellular levels. Here, we report a methodology to monitor lipid processing in ENTs of a living vertebrate. This in vivo approach is unique because intestinal lipid metabolism is observed in the presence of normal physiologic signals from the CNS and other organs, such as liver and vasculature.

We initially characterized the kinetics of FA absorption and metabolism by exposing larval ENTs to a meal rich in TG and cholesterol. We found FA derived from dietary TG were incorporated into TG-rich LDs, consistent with reports that, in the presence of excess lipid, TG storage is favored over lipoprotein export. We also found that absorption of dietary TG proceeds as a gradual and sustained (over 9 hr) accumulation in the ENT. These data suggest that intestinal lipid uptake is faster than lipid export, a process thought to be to be rate-limited.

While we performed a thorough TEM study of LD size and growth following feeding, we set out to develop methods to visualize lipid metabolism in live animals using fluorescent lipids. One such lipid, BODIPY-cholesterol, is known to behave similarly to cholesterol in both membrane partitioning and trafficking (Hölttä-Vuori et al., 2008; Marks et al., 2008; Wüstner et al., 2011). However, not all aspects of BODIPY-cholesterol subcellular transport have been examined and compared to native cholesterol. In comparison to NBD-cholesterol, BODIPY-cholesterol is brighter, more photo-stable, and more suitable for studying

uptake and inter-organelle sterol movement in living cells (Hölttä-Vuori et al., 2008; Wüstner et al., 2011). An unexpected finding of our study was that intestinal absorption of dietary cholesterol and FA are co-regulated. We ruled out the possibility that BODIPY-cholesterol was not absorbed because of a lack of phospholipase activity in the luminal intestine, which has been shown to reduce cholesterol absorption, perhaps by preserving the liquid-crystalline vesicles that can sequester cholesterol from micellar solubilization and thus from uptake by ENTs (Borgstrom, 1960; Huggins et al., 2003; Hui and Howles, 2005; Sylvén and Borgström, 1969; Young and Hui, 1999). This mechanism fails to explain why BODIPY-cholesterol emulsifications with exogenous bile, egg white, or BSA fail to be taken up into ENTs. Our results suggest that an additional factor, other than solubility, mediates intestinal cholesterol uptake. We provide evidence that either free FA or FA from dietary TG enhance luminal absorption of BODIPY-cholesterol.

Our observation that FA promotes intestinal cholesterol uptake are consistent with earlier studies conducted in rats that showed that efficiency of ENT cholesterol absorption is enhanced by feeding TG comprised of long-chain FA (Sylvén and Borgström, 1969). More recently, studies perfo[illegible] in mice (Hui and Howles, 2005) and zebrafish (Clifton et a[illegible] provided evidence consistent with a regulatory mechani[illegible] that links FA and cholesterol absorption. In zebrafish, pharmac[illegible] inhibition of cholesterol uptake (ezetimibe t[illegible]) interf[illegible] with intestinal absorption of both FA and fluores[illegible]nt chol[illegible]terol analog (Clifton et al., 2010). We[illegible]d that[illegible] ezetimi[illegible] analog (SCH58053) could block th[illegible] FA-[illegible] uptak[illegible] the BODIPY-cholesterol/egg white [illegible]. Here, w[illegible]ow specific FA modulate NPC1L1 localizatio[illegible] the BB, sug[illegible]ting that the mechanism triggering mo[illegible]ent[illegible]sponsive ma[illegible]ly to LCFA.

While we present evi[illegible]nce linking [illegible] and cholesterol absorption, we also found th[illegible]ese lipids are p[illegible]itioned into separate subcellular comp[illegible]ents s[illegible]n after uptake by ENTs. In zebrafish larvae, BO[illegible]Y-lab[illegible] and native FA are re-esterified to form TGs that are[illegible] incorp[illegible]ed into LDs (Figure 2; data not show[illegible]or wo[illegible]d e[illegible]lished that these BODIPY-FA are n[illegible]mpi[illegible]cting a[illegible] but are incorporated predominat[illegible] into ph[illegible]sphatidylch[illegible]oline and TG (Carten et al., 2011). The[illegible]ab[illegible]estinal BODIPY-FA observed in zebrafish la[illegible]s exactly what is expected from prior studies of mammalia[illegible]testinal FA metabolism.

Our data i[illegible]ate that cholesterol is initially transported via endosomes and, in contrast to FA, is only later (24 hr) found in some LDs (data not shown). BODIPY-cholesterol is esterified to cholesterol ester, albeit to a lesser degree than native cholesterol. However, native cholesterol competes with BODIPY-cholesterol for ester formation, suggesting that the same esterification pathway is utilized.

Interestingly, BODIPY-cholesteryl ester was detected only after modifying current extraction procedures (see Supplemental Experimental Procedures). Prior work in cultured cells observed a limited amount of BODIPY-cholesterol esterification that was not efficiently induced by acetylated LDL when compared to cells labeled with radioactive cholesterol (Hölttä-Vuori et al., 2008). Similarly, we observed less total BODIPY-cholesterol esterification as a percent of initial substrate than we found for [^{3}H]-cholesterol (data not shown). However, we did find a significant increase in BODIPY-cholesterol esterification in response to exogenous FA (Figures 3F and 3G). While these data are consistent with our hypothesis, they do not rule out the possibility that increased [^{3}H]-cholesterol and BODIPY-cholesterol esterification promoted by oleic acid[illegible] from enhanced intestinal acyl-CoA: cholesterol ac[illegible]nsferas[illegible]CAT) activity. Regardless, these data suggest[illegible] BODIPY-c[illegible]esterol can be processed by similar enzy[illegible]es as[illegible]lesterol a[illegible] its metabolism is promoted by FA. It[illegible]y very we[illegible] the[illegible]e that intestinal ACAT may be a ke[illegible]ediato[illegible]f this p[illegible]s.

Our observation th[illegible]holes[illegible]l absorption and trafficking within ENTs involves e[illegible]al tran[illegible]rt is consistent with prior studies o[illegible]olesterol[illegible]take[illegible]formed in heterologous cultured ce[illegible]s (CHO, 3[illegible]adipocytes, and McArdle-RH7777 [illegible]ato[illegible]ells) (Brown et al., 2007; Choudhury et al., 2002; Le Lay et a[illegible]006; Mukherjee et al., 1998; Yu et al., 200[illegible] propose tha[illegible]ward trafficking of cholesterol within t[illegible]endosomal compartment plays a central role in its absorp[illegible]n. However[illegible]e cannot exclude the possibility that some [illegible]ponent of[illegible]endosomal localization of BODIPY-cholesterol a[illegible] from r[illegible]se transport during cholesterol efflux (Storch et a[illegible]n contrast to cholesterol transport, we found no [illegible]vidence for FA transport through an endosomal compartment. [illegible]data not only support the widely held view that NPC1L1 functions as a sterol binding/transport protein, but they also advance previous assertions that the cellular processing of BODIPY-cholesterol is similar to that of native cholesterol.

Studies conducted in CaCo-2 cells support the view that levels of dietary cholesterol uptake into the ENT are in equilibrium with ENT membrane cholesterol (Field et al., 1998). Dietary cholesterol has also been proposed to stabilize ENT membranes following FA perfusion (Slota et al., 1983). Thus, it is conceivable that the co-regulation of FA and cholesterol absorption arose as a mechanism to protect ENTs from membrane damage caused by the absorption of free FA.

While the detailed mechanism of FA control of NPC1L1's localization awaits further study, our data indicate that cholesterol uptake requires the presence of luminal FA and occurs through the regulation of NPC1L1. Our finding that FA induce the relocation of a *Hs*NPC1L1-mCherry fusion protein from a resident perinuclear location to the apical cell membrane of the ENT provides one mechanism for linking cholesterol to FA uptake. Confirming that NPC1L1 subcellular dynamics observed with the fluorescent NPC1L1 fusion protein reflects that of endogenous NPC1L1 requires the development of better reagents. However, by exploiting these transgenic larvae to strongly overexpress NPC1L1, we were able to observe ENTs with significant NPC1L1 protein on the BB and FA-independent uptake of BODIPY-cholesterol. These data indicate that the localization of NPC1L1 to the BB is sufficient to facilitate luminal cholesterol uptake.

Although our findings regarding the role of NPC1L1 localization seem to contradict a recent study that presented evidence for transport of NPC1L1 from the apical cell membrane to the endosomal system of CaCo-2 and rat hepatoma cells during cholesterol absorption (Skov et al., 2011), this may be explained by the extensive methodological differences between the experimental approaches. The use of a live whole animal model is likely to capture important physiologic responses that will not

be apparent in ex vivo or in vitro approaches. For example, upon removal of cholesterol from culture media and cell membranes with a cholesterol depletion method (e.g., methyl-β-cyclodextrin), NPC1L1 is consistently found on the BB in CaCo-2 and McArdle RH7777 rat hepatoma cells (Chu et al., 2009; Ge et al., 2008; Wang et al., 2009; Yu et al., 2006). However, the low level of cholesterol achieved in these depleted cells may be well below that in a whole animal. When these depleted cells are bathed in a cholesterol-rich media (e.g., LPDS, compactin, mevalonate, and cholesterol/cyclodextrin for 1 hr), NPC1L1 relocates to a perinuclear compartment (Ge et al., 2008; Wang et al., 2009; Yu et al., 2006). Relocalization of NPC1L1 from the BB membrane has been proposed to play a protective role by preventing toxic levels of cholesterol uptake. It is worth noting that CaCo-2 and McArdle RH7777 rat hepatoma cells under "steady state" conditions are bathed in culture media rich in FA and cholesterol and, in those studies, NPC1L1 is also found in a perinuclear compartment (Davies et al., 2005; Yu et al., 2006). Furthermore, in porcine jejunum explants where cholesterol was not depleted, NPC1L1 was observed in an endosomal compartment after exposure to a cholesterol-rich media for 10 hr (Skov et al., 2011). Taken together, these data argue f odel where excess cholesterol triggers a protective respon e ing in removal of NPC1L1 from the BB.

In sum, we have developed and characterized a me d study intestinal ENT lipid uptake in an in g verte e, the larval zebrafish. This study provide sight to inte al cholesterol and FA uptake and rev that F rovide a ey relocalization signal for the subc llular 1L1. These data suggest a mechani o couple uptake of dietary cholesterol to FA availabi a the subc r localization of NPC1L1.

SIGNIFICANCE

Historically, zebr n has been largely used to study embryological ons an as been underutilized for studie hole a al p ology. To our knowledge, the wor esc ed in anuscript may be the first to v lize ve brate int tinal cholesterol absorption in vivo (c ini us, and symbiotes) at this level of reso .

Here, describe how to use the larval zebrafish for studies o gestive organ lipid metabolism by visualizing lipid trafficking at the subcellular level. We use this system to address a number of longstanding questions. For example, since the 1960s, it has been observed that dietary fat enhances cholesterol uptake but the mechanism underlying this effect has remained elusive. We found that the intestinal uptake of a fluorescent cholesterol analog (BODIPY-cholesterol) into an endosomal compartment is promoted by a common dietary long chain FA, oleic acid. We illustrate how to study the cell biology of this process by creating transgenic larval zebrafish that carry a human cholesterol transporter (NPC1L1) fused to the mCherry reporter. We found that oleic acid promotes the translocation of NPC1L1 to the brush border of the ENTs and that this translocation is sufficient to promote cholesterol uptake. These findings were not anticipated by prior cultured cell studies on NPC1L1 subcellular dynamics. The data presented demonstrate the power of the zebrafish larval system to provide fresh insights into the process of intestinal cholesterol absorption that cannot be elucidated in other model systems.

EXPERIMENTAL PROCEDURES

Animal Husbandry

Fish care and experimental cedures were pe per our Institutional Animal Care and Use Ap Protoc 39). Stand methods for breeding and raising zebrafish w fol d (Weste field, 2000). Embryos were obtained from na mati either w pe fish or transgenic lines. Embryos and l e used in e ment re raised at 28.5°C until 6 dpf when embr depleted.

High-Fat Diet

Fr nic EY was a to EM, vortexed, and forced pipetted for 5 min l lipid micelles formed ed at 0.5–4 μm diameter via confocal microspy). Six dpf larvae were fed the emulsion, either 10% (for electron microspy) or 5% (f orescence microscopy).

l Die

Larva d 3% puréed baby Artemia in EM overnight (8 hr).

at Diet

We designed a high-protein, fat-free diet by isolating and emulsifying the whites from chicken eggs. Larvae were fed a 5% solution of egg white.

FA Diet

Larvae were incubated with 1 mM oleic acid emulsified in either 5% egg white or 1% BSA.

Orlistat Treatment

To block generation of free FA from dietary triglycerides, larvae were pretreated with Orlistat (0.5 mM, 1 hr). After Orlistat pretreatment, half of the media was replaced with a 2× solution of the relevant diet and Orlistat.

Feeding the Diets

Larvae were moved to 12-well plastic dishes (20 larvae per well), provided with the relevant diet, and placed on a nutator (40 rpm) for various test durations. Larvae were rinsed from the diet solution four times in EM and moved to a watchglass where we determined feeding success by imaging under brightfield illumination (10×). The anterior larval intestine of most larvae was observed to be full of food, as evidenced by its opaque appearance.

Fluorescence Microscopy

Larvae were imaged with a Leica SP2 confocal microscope equipped with a 63× oil objective. The anterior intestine adjacent to the swim bladder, conservatively located in the zone of the anterior intestine (Wallace et al., 2005), was used for these studies (Figures 1A and 1B).

Electron Microscopy

For TEM, two feeding regimes were done. Larvae with "full" intestines were removed and fixed at different durations after feeding. The larvae were either fed overnight (8 hr) (as in Figure 1) or fed and sampled each hour from 1 to 21 hr post feeding (Figure S1). After four EM rinses, larvae were fixed in a 3% glutaraldyhyde, 1% formaldehyde, 0.1 M cacadylate solution. Postfixation was done in 1% osmium tetroxide and En Bloc-stained with uranyl acetate. Sections were made with an ultramicrotome (Porter-Blum MT-2; Sorvall Instruments, Newton, CT), mounted on Formvar-coated grids, and stained with lead citrate. Images were captured with a Phillips Tecnai 12 microscope and recorded with a Gatan multiscan CCD camera using Digital Micrograph software.

Mounting for In Vivo Imaging

Larvae were anesthetized with tricaine and moved to a bead of 3% methylcellulose solution. A 20 × 30 mm coverslip was used to hold the larvae in place. The wedge-shaped space created by the single slide bridge holds the larva's head in place during viewing (see Figure S3).

LD Area Quantification in Electron Micrographs

To define the rate of lipid processing, data were collected from several sets of animals from at least three independent experiments and tallied for overall lipid inclusion versus cell size over time using MetaMorph software (Molecular Devices, LLC, Sunnyvale, CA). For each larva (three per experiment), areas for all LDs within three separate cells were measured. Measurements of LD area were recorded by a program that we composed to recognize a set of defining features unique to LDs (a combination of shape factors and morphology filters). See Supplemental Experimental Procedures.

Analysis of Fluorescence within ENTs

A qualitative scoring method was devised, with a range from 0 to 5, and carried out by two independent researchers. The brightest signal observed within the ENT cytoplasm was given a score of 5 and absence of signal was scored 0. Images of three fields of cells, from three independent experiments, were blinded and scored.

MetaMorph software was used to measure fluorescence (relative fluorescence units) in ENTs in the anterior larval intestine adjacent to the swim bladder. Regions of interest (ROI) were chosen within the cytoplasmic space (excluding BB and nuclei) of at least 10 ENTs per individual animal which were measured for intensity.

Preparation of Fluorescent Lipid Suspensions

For BODIPY-FA labeling, 2.5 μl of a 2 μg/μl stock of F 2 (Invitrogen, Grand Island, NY) in chloroform was dried with gen gas, resuspended with 2.5 μl of 200-proof ethanol, and mixed with 100 EM. Twenty microliters of solution was added to 980 μl of EM (ml) plus dietary components where appropriate). For BODIPY sterol (Avanti Polar Lipids, Alabaster, AL) labeling, 4.6 μl similarly dried a 1.5 μg/μl stock solution, resuspended with 2.5 μl roof ethanol, and mixed with EM plus 1% FA-free BSA to ensure sion. Forty microliters of the suspension was added to 980 μl of EM (38 μg/ml) plus e (and dietary components where appropriate). When BODIPY labeled gs were added to the 5% EY emulsion, small celles (0.5 μm–4 μm diameter) were labeled. When analogs were added the 5% white emulsion, a uniform emulsion was formed.

Extraction of Lipids

To purify and metabolites from fed various diets containing either [^{3}H]-cholesterol ([1,2-N)]) 50 Ci/mmol Perkin Elmer or BODIPY-cholesterol, lipid extracts 10 larvae prepared using a modified extraction method (Bligh and , 1959) (full protocol provided in Supplemental Experimental Procedures). Larvae were washed and sonicated (1 min) in EM (1 ml). Four milliliters of chloroform/methanol solution (1:2) was added to sonicated larvae in stages. Following extraction, the organic layer was dried, reconstituted in 100% chloroform, and stored at −80°C.

Thin Layer Chromatography

To resolve [^{3}H]-cholesterol and fluorescent cholesterol metabolites (cholesterol, cholesterol ester, and BODIPY493/503) by TLC, a petroleum ether, ethyl ether, acetic acid (80:20:1) solvent system was employed. Solvents were mixed, added to TLC chambers, and allowed to equilibrate (20 min). Samples and BODIPY standards were spotted onto silica gel TLC plates (Whatman, LK5D; EMD Biochemicals) and dried (15 min). Detection of fluorescent bands was performed on a Storm Scanner 860 (Molecular Dynamics, USA) using a blue fluorescence laser (excitation: 450 nm; emission: 520LP; PMT 800V, 200μ pixel size). Plates containing radioactive lipids were scanned using an AR-2000 (Bioscan, USA).

Endocytic Compartment Labeling

Six dpf larvae were immersed in 0.22 mM AM1-43 (Molecular Probes) in EM for 1 hr. For labeling with transferrin from human serum, Alexa-Fluor 555 (Invitrogen, Grand Island, NY), larvae were pretreated with a 1× solution of cOmplete, Mini Protease Inhibitor Cocktail Tablets (Roche Diagnostics) in EM for 1 hr and then immersed in a diet solution including 1× protease inhibitor, 0.4 mg/ml transferrin 555, and 5% EY for 3 hr. Larvae were rinsed in EM four times prior to imaging.

Co-Localization Analysis

Co-localization analysis of fluorescent ma was performe ImarisColoc software (Bitplane) and was based on the sion of int ity pairs that exhibit no correlation (Pearson' rrelation zero) thresholded Manders' coefficients (Coste al., 2004; Ima Manders et al., 1993) (Supplemental Expe tal Pro res).

Construction of Hu n NP nCherry ion Vector

To make a huma C1L1-mC fusio nstruct under the control of a heat shock ter (*hsp70-Hs nCherry*), we designed a Tol2 construct a Ky t al. (2007). *HsNPC1L1-GFP* tagged construct (from J.P. Davies, Mo inai School of Medicine, NY) was modified to be driven by the heat shock oter *hsp70* and to replace GFP with mCherry. St were derived us *hsp70-hsNPC1L1:mCherry* constructs using insertion. Larvae were heat shocked either 15 min (clonal experiments) hr (stable line periments), allowed to recover and express the transgene , and then m d to various diets.

Sta sis

Data in ba graphs are expressed as mean ± SEM. Statistical analyses shown main figures were performed using SPSS. Comparisons were made two-tailed t test for equality of means (Figures 2, 3G, and 3H) or analysis of variance (ANOVA; Figures 3F, 3I, 3J, 5, and 6); all were preceded by the Levene test for equality of variances. Outcome of each Levene test determined whether ANOVA was followed up with the post-hoc procedure Ryan-Einot-Gabriel-Welsch range (equal variances assumed) or Games-Howell (equal variances not assumed). Shown in Figure S1B and S1D, linear regression was performed using R version 2.14 (http://www.r-project.org). In both analyses, linear regression of log-average LD area versus time post feed was performed, and the best model was selected using the Akiake Information Criteria. Generalized additive models where log-average LD area could vary as a smooth spline of time post feed were also fit to the data (Figure S1B). A p value < 0.05 was considered statistically significant.

SUPPLEMENTAL INFORMATION

Supplemental Information contains four figures and Supplemental Experimental Procedures and can be found with this article online at doi:10.1016/j.chembiol.2012.05.018.

ACKNOWLEDGMENTS

The authors are grateful to Mike Sepanski who provided invaluable help with electron microscopy. This work was funded by grants from the NIH (R56DK093399 and RO1GM63904 to S.A.F.; RO1DK54942 to M.P.; HL083187 to R.B.; and F32DK081308 to J.W.W.) and the American Heart Association (0825406E to J.W.W.). Additional funding was provided to S.A.F. by the G. Harold and Leila Y. Mathers Charitable Foundation and the Carnegie Institution for Science endowment. S.A.F. and M.P. are inventors on a patent describing the use of fluorescent lipids for drug discovery in zebrafish. The patent is the property of the Carnegie Institution and the University of Pennsylvania. R.B. is an inventor on a patent on BODIPY-cholesterol that is the property of the Research Foundation of CUNY, and all rights accruing to the patent holder have been assigned to CUNY, the institution that employs R.B. We would also like to thank Nicholas Ingolia and Justin Lessler for helpful discussions regarding statistics and Marnie Halpern for critical reading of the manuscript.

Received: May 31, 2011
Revised: May 24, 2012
Accepted: May 31, 2012
Published online: June 28, 2012

REFERENCES

Altmann, S.W., Davis, H.R., Jr., Zhu, L.J., Yao, X., Hoos, L.M., Tetzloff, G., Iyer, S.P., Maguire, M., Golovko, A., Zeng, M., et al. (2004). Niemann-Pick C1 Like 1 protein is critical for intestinal cholesterol absorption. Science *303*, 1201–1204.

André, M., Ando, S., Ballagny, C., Durliat, M., Poupard, G., Briançon, C., and Babin, P.J. (2000). Intestinal fatty acid binding protein gene expression reveals the cephalocaudal patterning during zebrafish gut morphogenesis. Int. J. Dev. Biol. *44*, 249–252.

Ashworth, C.T., and Lawrence, J.F. (1966). Electron microscopic study of the role of lipid micelles in intestinal fat absorption. J. Lipid Res. *7*, 465–472.

Babin, P.J., Thisse, C., Durliat, M., Andre, M., Akimenko, M.A., and Thisse, B. (1997). Both apolipoprotein E and A-I genes are present in a nonmammalian vertebrate and are highly expressed during embryonic development. Proc. Natl. Acad. Sci. USA *94*, 8622–8627.

Babitt, J., Trigatti, B., Rigotti, A., Smart, E.J., Anderson, R.G., Xu, S., and Krieger, M. (1997). Murine SR-BI, a high density lipoprotein receptor that mediates selective lipid uptake, is N-glycosylated and fatty acylated and colocalizes with plasma membrane caveolae. J. Biol. Chem. *272*, 13242–13249.

Benzonana, G., and Desnuelle, P. (1965). Kinetic study of the action of pancreatic lipase on emulsified triglycerides. Enzymology assay in heterogeneous medium. Biochim. Biophys. Acta *105*, 121–136.

Betz, W.J., Mao, F., and Bewick, G.S. (1992). Activity-dependent [illegible] staining and destaining of living vertebrate motor nerve [illegible]minal. J. Neurosci. *12*, 363–375.

Bidet, M., Joubert, O., Lacombe, B., Ciantar, M., [illegible] R., Mo[illegible]., Brétillon, L., Faure, H., Bittman, R., Ruat, M., and [illegible]s-ve[illegible], I. (201[illegible]. The hedgehog receptor patched is involved in ch[illegible]erol tra[illegible]ort. PLoS [illegible]E *6*, e23834.

Bligh, E.G., and Dyer, W.J. (1959). A ra[illegible] metho[illegible] lipid extraction and purification. Can. J. Biochem. Physi[illegible], 911–917.

Borgstrom, B. (1960). Studies [illegible]inal cholester[illegible]sorption in the human. J. Clin. Invest. *39*, 80[illegible]5.

Brown, J.M., Rudel, L.L., and Yu, L. (2007). [illegible]L1 (Niemann-Pick C1-like 1) mediates sterol-spec[illegible]unidirectional transpo[illegible]non-esterified cholesterol in McArdle-RH777[illegible]patoma[illegible]s. Biochem. J. *406*, 273–283.

Carten, J.D., Bra[illegible], M[illegible]and Farber, S.A. (2011). Visualizing digestive organ morphology a[illegible]ction usi[illegible]fferential fatty acid metabolism in live zeb[illegible]v. Bio[illegible]276[illegible].

Che[illegible], Li, Q.[illegible]ang, Y., [illegible]., Zong, Y., Qu, S., and Liu, Z. (2011). Oleic a[illegible]decreas[illegible]ne expression of a cholesterol transport-related protein (N[illegible]) h[illegible]f endoplasmic reticulum stress in CaCo-2 cells. J. Phy[illegible]iochem. *67*, 153–163.

Choudhur[illegible]Dominguez, M., Puri, V., Sharma, D.K., Narita, K., Wheatley, C.L., Marks, [illegible]and Pagano, R.E. (2002). Rab proteins mediate Golgi transport of caveola-internalized glycosphingolipids and correct lipid trafficking in Niemann-Pick C cells. J. Clin. Invest. *109*, 1541–1550.

Chu, B.B., Ge, L., Xie, C., Zhao, Y., Miao, H.H., Wang, J., Li, B.L., and Song, B.L. (2009). Requirement of myosin Vb.Rab11a.Rab11-FIP2 complex in cholesterol-regulated translocation of NPC1L1 to the cell surface. J. Biol. Chem. *284*, 22481–22490.

Clifton, J.D., Lucumi, E., Myers, M.C., Napper, A., Hama, K., Farber, S.A., Smith, A.B., 3rd, Huryn, D.M., Diamond, S.L., and Pack, M. (2010). Identification of novel inhibitors of dietary lipid absorption using zebrafish. PLoS ONE *5*, e12386.

Costes, S.V., Daelemans, D., Cho, E.H., Dobbin, Z., Pavlakis, G., and Lockett, S. (2004). Automatic and quantitative measurement of protein-protein colocalization in live cells. Biophys. J. *86*, 3993–4003.

Davies, J.P., Scott, C., Oishi, K., Liapis, A., and Ioannou, Y.A. (2005). Inactivation of NPC1L1 causes multiple lipid transport defects and protects against diet-induced hypercholesterolemia. J. Biol. Chem. *280*, 12710–12720.

Davies, J.P., and Ioannou, Y.A. (2006). The role of the Niemann-Pick C1-like 1 protein in the subcellular transport of multiple lipids and their homeostasis. Curr. Opin. Lipidol. *17*, 221–226.

Diefenbach, T.J., Guthrie, P.B., Stier, H., Billups, B., and Kater, S.B. (1999). Membrane recycling in the neuronal growth co[illegible]led by FM1-43 labeling. J. Neurosci. *19*, 9436–9444.

Durliat, M., André, M., and Babin, P.J. [illegible]0). Conserve[illegible]otein motifs and structural organization of a fish gene ho[illegible]ous to mam[illegible]an apolipoprotein. E. Eur. J. Biochem. *267*, 54[illegible]59.

Farber, S.A., De Rose, R.A., [illegible], E.S., and H[illegible], M[illegible](2003). The zebrafish annexin gene family. [illegible]me Res[illegible](6A), [illegible]96.

Field, F.J. (2001). Regula[illegible]of int[illegible]al cholesterol metabolism. In Intestinal Lipid Metabolism, [illegible]M. Ma[illegible], P. Tso, [illegible]A. Kuksis, eds. (New York: Kluwer Academi[illegible]p. 235–25[illegible].

Field, F.J., B[illegible], Murthy, S., an[illegible], S.N. (1998). Transport of cholesterol from [illegible]en[illegible]smic reticulum [illegible]the plasma membrane is constitutive in CaCo-2 cells and [illegible] from the transport of plasma membrane cholesterol to th[illegible]doplasmic reti[illegible]. J. Lipid Res. *39*, 333–343.

[illegible], H.A., Dong, P.D., Be[illegible]D., and Stainier, D.Y. (2003). Formation of the [illegible]gestive system in zebrafish. II. Pancreas morphogenesis. Dev. Biol. *261*, [illegible]97–208.

[illegible]barino, J., [illegible]amsee, M., Wilcox, L., Oelkers, P.M., D'Ambrosio, D., [illegible]s, K.V., [illegible]msey, N., Jabado, O., Turkish, A., and Sturley, S.L. (2009). Ste[illegible]ylglycerol acyltransferase deficiency triggers fatty acid-mediated cell death. J. Biol. Chem. *284*, 30994–31005.

[illegible]Wang, J., Qi, W., Miao, H.H., Cao, J., Qu, Y.X., Li, B.L., and Song, B.L. (2008). The cholesterol absorption inhibitor ezetimibe acts by blocking the sterol-induced internalization of NPC1L1. Cell Metab. *7*, 508–519.

Hama, K., Provost, E., Baranowski, T.C., Rubinstein, A.L., Anderson, J.L., Leach, S.D., and Farber, S.A. (2009). In vivo imaging of zebrafish digestive organ function using multiple quenched fluorescent reporters. Am. J. Physiol. Gastrointest. Liver Physiol. *296*, G445–G453.

Hendrickson, H.S., Hendrickson, E.K., Johnson, I.D., and Farber, S.A. (1999). Intramolecularly quenched BODIPY-labeled phospholipid analogs in phospholipase $A_{(2)}$ and platelet-activating factor acetylhydrolase assays and in vivo fluorescence imaging. Anal. Biochem. *276*, 27–35.

Ho, S.Y., Thorpe, J.L., Deng, Y., Santana, E., DeRose, R.A., and Farber, S.A. (2004). Lipid metabolism in zebrafish. Methods Cell Biol. *76*, 87–108.

Ho, S.Y., Lorent, K., Pack, M., and Farber, S.A. (2006). Zebrafish fat-free is required for intestinal lipid absorption and Golgi apparatus structure. Cell Metab. *3*, 289–300.

Hölttä-Vuori, M., Uronen, R.L., Repakova, J., Salonen, E., Vattulainen, I., Panula, P., Li, Z., Bittman, R., and Ikonen, E. (2008). BODIPY-cholesterol: a new tool to visualize sterol trafficking in living cells and organisms. Traffic *9*, 1839–1849.

Hölttä-Vuori, M., Salo, V.T., Nyberg, L., Brackmann, C., Enejder, A., Panula, P., and Ikonen, E. (2010). Zebrafish: gaining popularity in lipid research. Biochem. J. *429*, 235–242.

Huggins, K.W., Camarota, L.M., Howles, P.N., and Hui, D.Y. (2003). Pancreatic triglyceride lipase deficiency minimally affects dietary fat absorption but dramatically decreases dietary cholesterol absorption in mice. J. Biol. Chem. *278*, 42899–42905.

Hui, D.Y., and Howles, P.N. (2005). Molecular mechanisms of cholesterol absorption and transport in the intestine. Semin. Cell Dev. Biol. *16*, 183–192.

Imaris. (2007). Imaris software V 6.0. Bitplane AG (http://www.bitplane.com/go/products/imariscoloc).

Iqbal, J., Dai, K., Seimon, T., Jungreis, R., Oyadomari, M., Kuriakose, G., Ron, D., Tabas, I., and Hussain, M.M. (2008). IRE1beta inhibits chylomicron production by selectively degrading MTP mRNA. Cell Metab. *7*, 445–455.

Iqbal, J., and Hussain, M.M. (2009). Intestinal lipid absorption. Am. J. Physiol. Endocrinol. Metab. *296*, E1183–E1194.

Ish-Horowicz, D., Holden, J.J., and Gehring, W.J. (1977). Deletions of two heat-activated loci in Drosophila melanogaster and their effects on heat-induced protein synthesis. Cell *12*, 643–652.

Jersild, R.A., Jr. (1966). A time sequence study of fat absorption in the rat jejunum. Am. J. Anat. *118*, 135–162.

Klett, E.L., and Patel, S.B. (2004). Biomedicine. Will the real cholesterol transporter please stand up. Science *303*, 1149–1150.

Kruit, J.K., Groen, A.K., van Berkel, T.J., and Kuipers, F. (2006). Emerging roles of the intestine in control of cholesterol metabolism. World J. Gastroenterol. *12*, 6429–6439.

Kuromi, H., and Kidokoro, Y. (2005). Exocytosis and endocytosis of synaptic vesicles and functional roles of vesicle pools: lessons from the Drosophila neuromuscular junction. Neuroscientist *11*, 138–147.

Kwan, K.M., Fujimoto, E., Grabher, C., Mangum, B.D., Hardy, M.E., Campbell, D.S., Parant, J.M., Yost, H.J., Kanki, J.P., and Chien, C.B. (2007). The Tol2kit: a multisite gateway-based construction kit for Tol2 transposon transgenesis constructs. Dev. Dyn. *236*, 3088–3099.

Labonté, E.D., Camarota, L.M., Rojas, J.C., Jandacek, R.J., Gilham, D.E., Davies, J.P., Ioannou, Y.A., Tso, P., Hui, D.Y., and Howles, P.N. (2008). Reduced absorption of saturated fatty acids and resistance to diet-induced obesity and diabetes by ezetimibe-treated and Npc1l1-/- mice. Am. J. Physiol. Gastrointest. Liver Physiol. *295*, G776–G783.

Le Lay, S., Hajduch, E., Lindsay, M.R., Le Lièpvre, X., Thiele, C., Ferré, P., Parton, R.G., Kurzchalia, T., Simons, K., and Dugail, I. (2006). Cholesterol-induced caveolin targeting to lipid droplets in adipocytes: a role for caveolar endocytosis. Traffic *7*, 549–561.

Lehner, R., and Kuksis, A. (1995). Triacylglycerol synthesis by purifi[ed] [di]acylglycerol synthetase of rat intestinal mucosa. Role of acyl-CoA acyltr[ansferase]. J. Biol. Chem. *270*, 13630–13636.

Li, Z., Mintzer, E., and Bittman, R. (2006). First synthesis of free chol[esterol]-BODIPY conjugates. J. Org. Chem. *71*, 1718–1721.

Manders, E., Verbeek, F., and Aten, J. (1993). Mea[surement] of co-localiza[tion] of objects in dual-colour confocal images. J. Mi[crosc.] *169*, 3[75]–382.

Mansbach, C.M., 2nd, and Gorelick, F. (2007). De[velopmental] me[chani]cal regulation of intestinal lipid absorption. [Die]tary [tri]sorption, complex lipid synthesis, and the intracellular pa[cka]ging and sec[retion] of chylomicrons. Am. J. Physiol. Gastrointest. Liver [Physiol.] *293*, G645–G6[56].

Mansbach, C.M., 2nd, and Nevi[n, P.] (199[5]). Intracellular movement of triacylglycerols in the intestine. J. [Lip]id Res. *39*, 9[63]–978.

Mansbach, C.M., and S[iddiqi], S.A. (2010). The [bio]genesis of chylomicrons. Annu. Rev. Physiol. [72], 315–333.

Marenus, K.D., and [Strand], S. (1982). Sequence of structural changes in columnar epithelium [of] intestine [dur]ing early stages of fat absorption. J. Ultrastru[ct. Res.] *79*, 9[2–]

Marks, [D.], Bit[tman], R., a[nd] [Pa]go, R.E. (2008). Use of Bodipy-labeled sphi[n]golipid and [ch]olesterol a[na]logs to examine membrane microdomains in c[ultured] fibroblasts. Traffic *130*, 819–832.

Martin, [F.P.], [Wa]ng, Y., Sp[ren]ger, N., Yap, I.K., Lundstedt, T., Lek, P., Rezzi, S., Ramadan, [Z.], [Van] Bladeren, P., Fay, L.B., et al. (2008). Probiotic modulation of symbiotic gu[t] microbial-host metabolic interactions in a humanized microbiome mouse m[odel]. Mol. Syst. Biol. *4*, 157.

Marza, E., Barthe, C., André, M., Villeneuve, L., Hélou, C., and Babin, P.J. (2005). Developmental expression and nutritional regulation of a zebrafish gene homologous to mammalian microsomal triglyceride transfer protein large subunit. Dev. Dyn. *232*, 506–518.

Moschetta, A., Xu, F., Hagey, L.R., van Berge-Henegouwen, G.P., van Erpecum, K.J., Brouwers, J.F., Cohen, J.C., Bierman, M., Hobbs, H.H., Steinbach, J.H., and Hofmann, A.F. (2005). A phylogenetic survey of biliary lipids in vertebrates. J. Lipid Res. *46*, 2221–2232.

Mukherjee, S., Zha, X., Tabas, I., and Maxfield, F.R. (1998). Cholesterol distribution in living cells: fluorescence imaging using dehydroergosterol as a fluorescent cholesterol analog. Biophys. J. *75*, 1915–1925.

Murthy, V.N., and Stevens, C.F. (1998). Synaptic vesicles retain their identity through the endocytic cycle. Nature *392*, 497–501.

Ng, A.N., de Jong-Curtain, T.A., Mawdsley, D.J., White, S.J., Shin, J., Appel, B., Dong, P.D., Stainier, D.Y., and Heath, J.K. (2005). Formation of the digestive system in zebrafish: III. Intestinal epithelium morphogenesis. Dev. Biol. *286*, 114–135.

Nutting, D., Hall, J., Barrowman, J.A., and Tso, P. (1989). Further studies on the mechanism of inhibition of intestinal chylomicron transport by Pluronic L-81. Biochim. Biophys. Acta *1004*, 357–362.

O'Rourke, E.J., Soukas, A.A., Carr, C.E., [Gu]avkuri, [G.] (2009). C. elegans major fats are stored in vesicles distinct [fr]om lysosome-[re]lated organelles. Cell Metab. *10*, 430–435.

Pack, M., Solnica-Krezel, L., M[ull]i, J., [Ha]uss, S. [Ma]Schier, A.F., Stemple, D.L., Driever, W., an[d] [Fi]shman, M.C. [19]96). Mutations affecting development of zebrafish di[ges]tive orga[n] Develop[ment] *23*, 321–328.

Sankaranarayanan, S., Ké[kes]Weibe[l], de la Llera-Moya, M., Phillips, M.C., Asztalos, B.F., Bittm[an], R., a[nd] [Ro]blat, G.H[.] (2011). A sensitive assay for ABCA1-mediated [ch]olesterol ef[flux] using B[ODIPY]-cholesterol. J. Lipid Res. *52*, 2332–2340.

Sarda, L., a[nd] [Des]nuelle, P. (1958). Ac[tio]n of pancreatic lipase on esters in emulsions. Biochim. B[iophys.] Acta *30*, 513–521.

Sire, M[arie]-J[ean] Sutton, C., and [Ire]land, J.M. (1981). New views on intestinal absorption of lipi[d]s in teleostean fish[es]: an ultrastructural and biochemical study in the rainbow trout. J. Lipid Res. *22*, 81–94.

Sø[rens]v, M., Tønne[sen], C.K., Hansen, G.H., and Danielsen, E.M. (2011). Dietary cholesterol induc[es] trafficking of intestinal Niemann-Pick Type C1 Like 1 fro[m] brush[-]border to endosomes. Am. J. Physiol. Gastrointest. Liver Physi[ol.] [30]–G40.

[Ta]ta, T., Kozlov, N.A., and Ammon, H.V. (1983). Comparison of cholesterol [and] sitosterol: effects on jejunal fluid secretion induced by oleate, and absorption from mixed micellar solutions. Gut *24*, 653–658.

Storch, C.H., Ehehalt, R., Haefeli, W.E., and Weiss, J. (2007). Localization of the human breast cancer resistance protein (BCRP/ABCG2) in lipid rafts/caveolae and modulation of its activity by cholesterol in vitro. J. Pharmacol. Exp. Ther. *323*, 257–264.

Sylvén, C., and Borgström, B. (1969). Intestinal absorption and lymphatic transport of cholesterol in the rat: influence of the fatty acid chain length of the carrier triglyceride. J. Lipid Res. *10*, 351–355.

Titus, E., and Ahearn, G.A. (1992). Vertebrate gastrointestinal fermentation: transport mechanisms for volatile fatty acids. Am. J. Physiol. *262*, R547–R553.

Tremblay, A.J., Lamarche, B., Lemelin, V., Hoos, L., Benjannet, S., Seidah, N.G., Davis, H.R., Jr., and Couture, P. (2011). Atorvastatin increases intestinal expression of NPC1L1 in hyperlipidemic men. J. Lipid Res. *52*, 558–565.

U.S. Department of Agriculture, Agricultural Research Service. (2011). USDA National Nutrient Database for Standard Reference, Release 24. Nutrient Data Laboratory Home Page, http://www.ars.usda.gov/ba/bhnrc/ndl.

Wallace, K.N., Akhter, S., Smith, E.M., Lorent, K., and Pack, M. (2005). Intestinal growth and differentiation in zebrafish. Mech. Dev. *122*, 157–173.

Wang, J., Chu, B.B., Ge, L., Li, B.L., Yan, Y., and Song, B.L. (2009). Membrane topology of human NPC1L1, a key protein in enterohepatic cholesterol absorption. J. Lipid Res. *50*, 1653–1662.

Weiss, J.M. (1955). The role of the Golgi complex in fat absorption as studied with the electron microscope with observations on the cytology of duodenal absorptive cells. J. Exp. Med. *102*, 775–782.

Westerfield, M. (2000). The zebrafish book. A guide for the laboratory use of zebrafish (D. Rerio), Fourth Edition (Eugene, OR: University of Oregon Press).

Wüstner, D., Solanko, L., Sokol, E., Garvik, O., Li, Z., Bittman, R., Korte, T., and Herrmann, A. (2011). Quantitative assessment of sterol traffic in living cells by dual labeling with dehydroergosterol and BODIPY-cholesterol. Chem. Phys. Lipids *164*, 221–235.

Young, S.C., and Hui, D.Y. (1999). Pancreatic lipase/colipase-mediated triacylglycerol hydrolysis is required for cholesterol transport from lipid emulsions to intestinal cells. Biochem. J. *339*, 615–620.

Yu, L., Bharadwaj, S., Brown, J.M., Ma, Y., Du, W., Davis, M.A., Michaely, P., Liu, P., Willingham, M.C., and Rudel, L.L. (2006). Cholesterol-regulated translocation of NPC1L1 to the cell surface facilitates free cholesterol uptake. J. Biol. Chem. *281*, 6616–6624.